Supplemental Materials

Molecular Biology of the Cell

Hernandez et al.

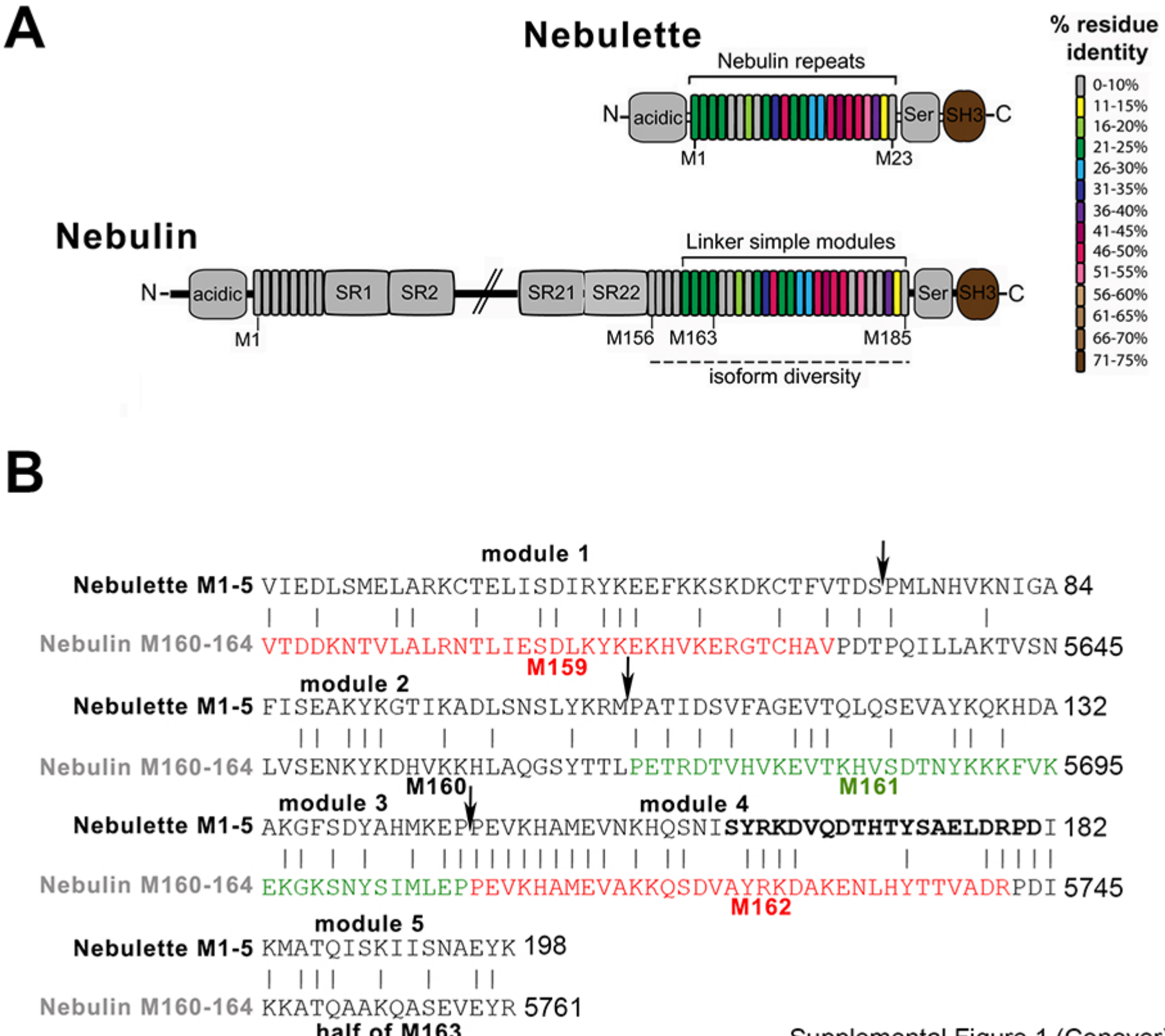

Supplemental Figure 1 (Conover)

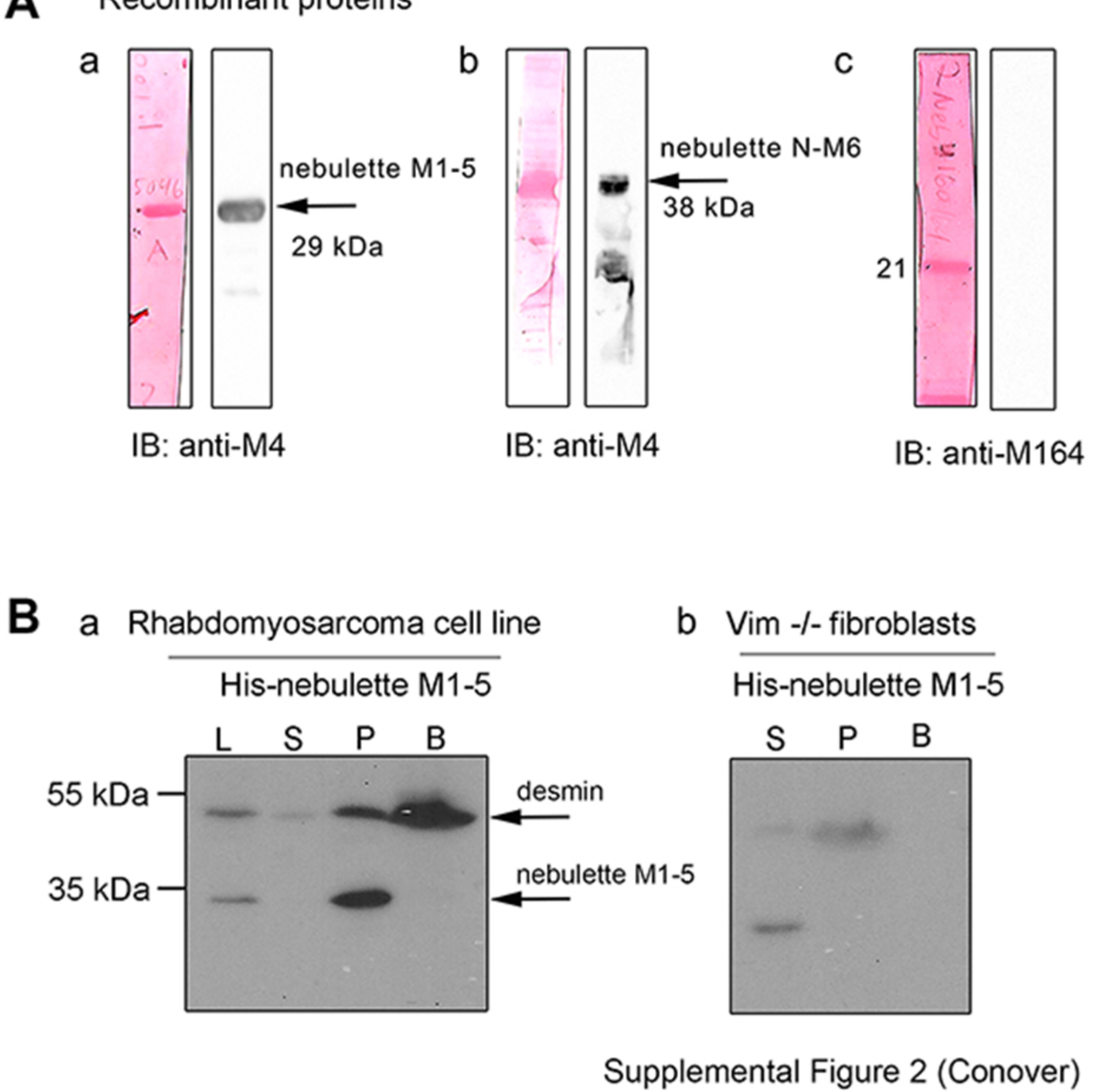
A
Recombinant proteins
a
nebulette M1-5
29 kDa
IB: anti-M4
b
nebulette N-M6
38 kDa
IB: anti-M4
c
21
IB: anti-M164
B
a Rhabdomyosarcoma cell line
His-nebulette M1-5
L S P B
55 kDa
35 kDa
desmin
nebulette M1-5
b Vim -/- fibroblasts
His-nebulette M1-5
S P B
Supplemental Figure 2 (Conover)

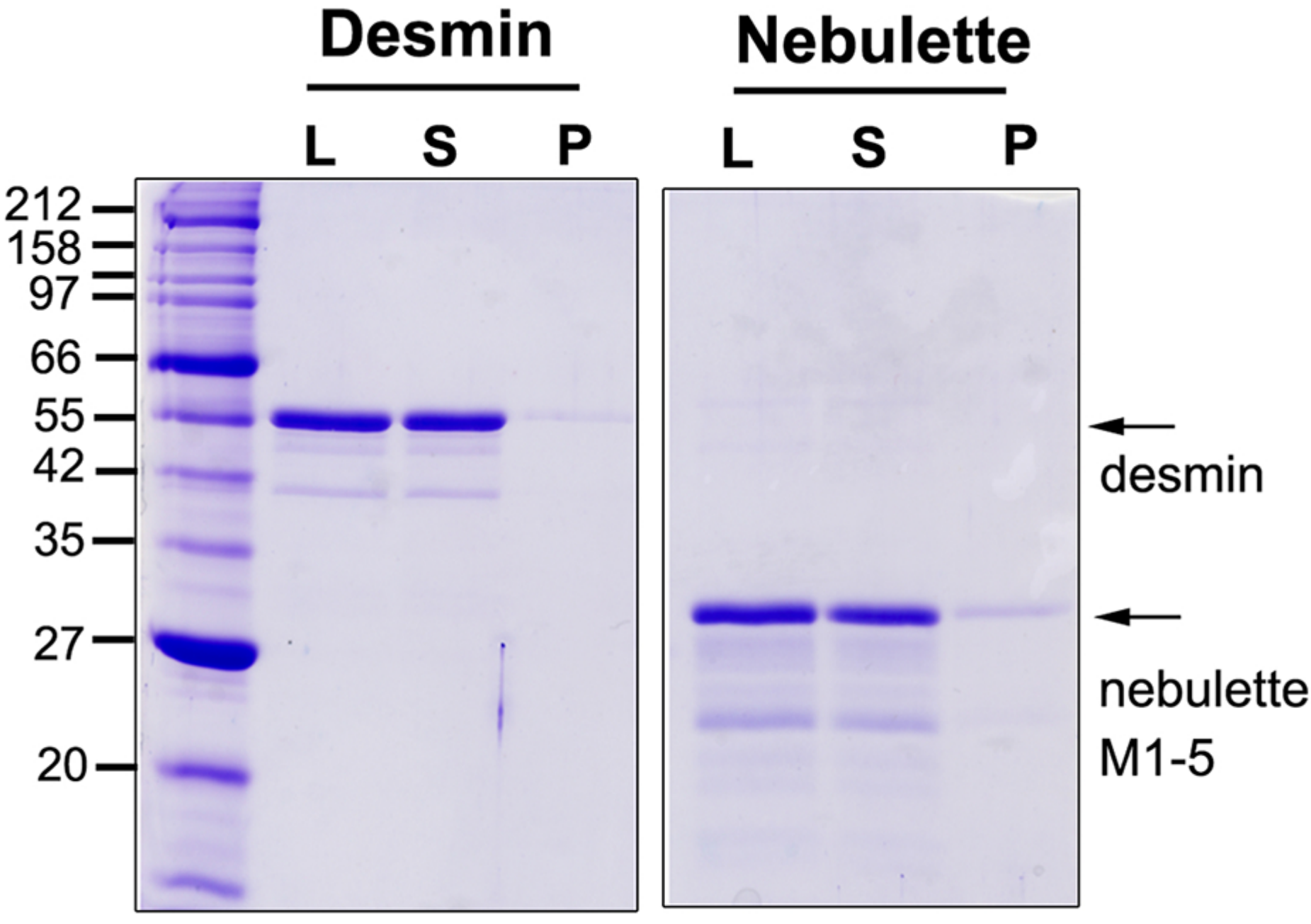

Supplemental Figure 3 (Conover)

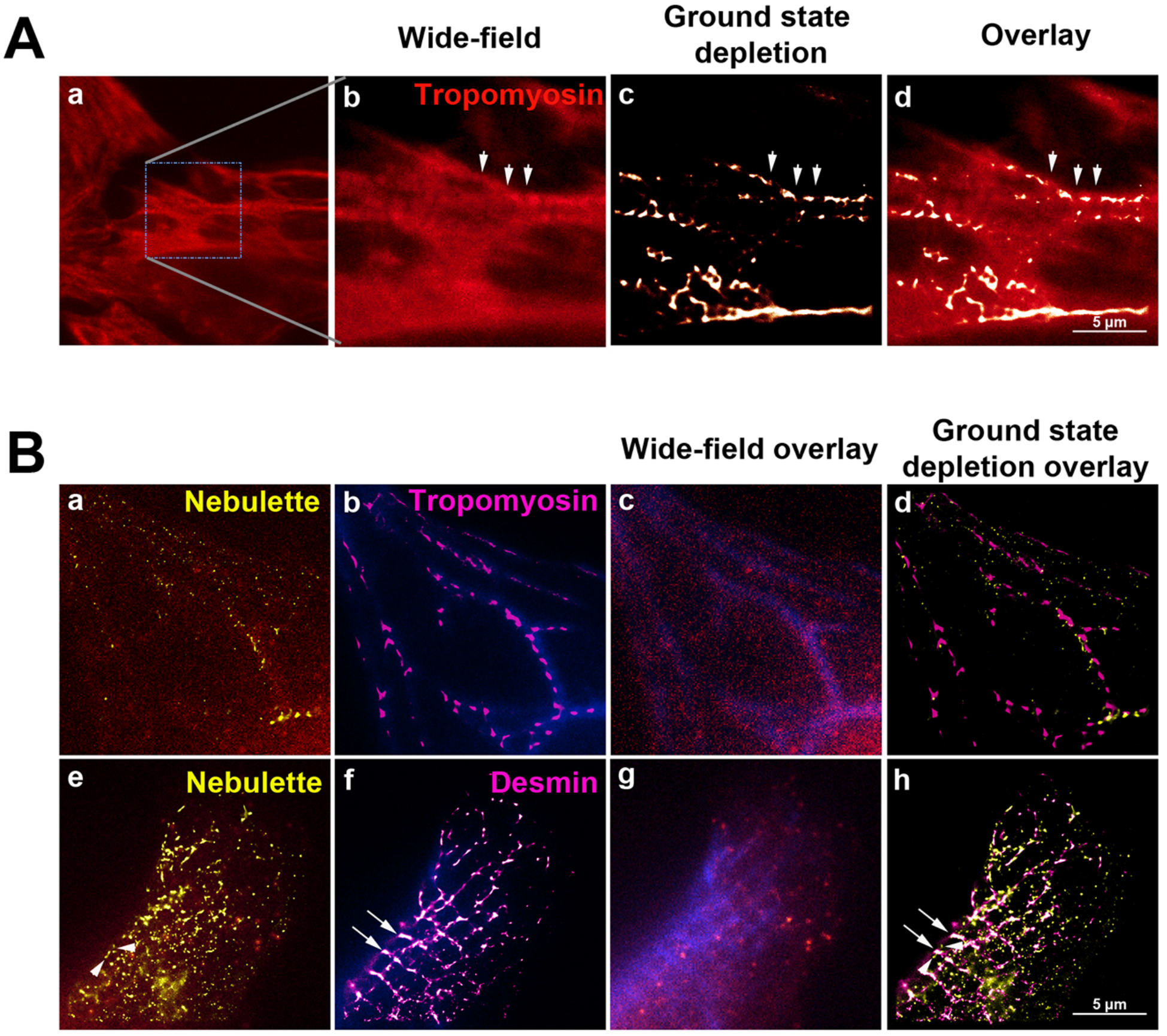

Supplemental Figure S4 (Conover)

Supplemental Figure Legends

Supplemental Figure 1. Molecular organization and sequence alignments of nebulette and nebulin. (A) Nebulin modules160 through 181 were used for the alignment against all of nebulette modules. Nebulette isoform X4 (~100-109 kDa, pI 9.38) has a glutamate domain, 23 modules or nebulin-like repeats (modules 1-23), and serine and SH3 domains. Nebulin (~600-900 kDa, pI 9.72) is large modular protein organized as follows: glutamate domain, single repeats (modules 1-8), super-repeats (SR1-22, containing WLKGIGW motif at the end of the third repeat of each SR, each SR is formed by groups of 7 single repeats modules 9-162 that are spatially matched to the 7-actin monomers), single repeats (modules 163-185), and serine and SH3 domains. Single modules consist of 35 amino-acid alpha-helical repeats with a conserved SDxxYK motif binds F-actin. Shown are color-coded % residue identities for all nebulette modules against nebulin modules 160-185 as determined by BLASTp. Modules boundaries for nebulette aligned against nebulin used in the schematic were defined by (Moncman and Wang, 2000). (B) Primary amino-acid sequence alignment of human nebulin modules M160-164 and human nebulette modules M1-5. The nebulette antigen spanning residues 162-181 (SYRKDVQDTHTYSAELDRPD, highlighted in a black box) used to generate the nebulette M4 antibodies has a low residue identity to nebulin and high antigenicity. Arrows point to the module boundaries in nebulette according to (Millevoi *et al.*, 1998), and in nebulin according to (Labeit and Kolmerer, 1995) nomenclature.

Supplemental Figure 2. Immunoprecipitation of endogenous desmin in rhabdomyosarcoma skeletal muscle cells transiently expressing nebulette M1-5. (A) His-tagged recombinant nebulette proteins were probed in a Western blot using anti-nebulette M4 antibodies. A band migrating at ~29 kDa corresponds to the predicted size of the nebulette fragment encompassing modules 1 through 5 (Aa), and a ~38 kDa band corresponding to the predicted size of nebulette fragment expressing the amino terminus through module M6 (Ab). No crossreacting nebulette band was detected when recombinant nebulin modules 160-164 protein was probed (Ac). (B) Co immunoprecipitation assay and Western blot using anti-His antibodies detect a band migrating below 55 kDa that corresponds to endogenous desmin molecular weight in rhabdomyosarcoma cell soluble lysates transiently expressing pIRES His-nebulette M1-5 (Bead lane, Ba). In contrast, no bands were detected in the bead sample of vimentin$^{-/-}$ fibroblasts expressing pIRES His-nebulette M1-5 (Bb). Abbreviations: L = lysate, S = supernatant, P = pellet, B = IgA beads.

Supplemental Figure 3. Recombinant full-length desmin and nebulette M1-5 proteins. (A) Coomassie brilliant blue stained SDS-PAGE gels show the purity and the fractionation of soluble desmin and nebulette from non-specific aggregates. This was achieved using a 30 min ultracentrifugation (Beckman airfuge 100000 xg, 30 psi). These proteins were used in co-sedimentation experiments. Abbreviations: total protein load = L, soluble protein= S and pellet = P.

Supplemental Figure 4. Localization of nebulette module 4 in actin filaments in *ex vivo* cardiomyocytes. A ~60 µm box imaged by WF microscopy in fixed cells stained for tropomyosin using a red fluorophore is shown in panel Aa. A ~20 µm smaller box within

this cell was selected for imaging by super resolution GSD microscopy (Ab). Notice that the GSD image improves the resolution of tropomyosin (Ac) as compared to WF. An overlay of both WF and GSD images are displayed for comparison (Ad, red and white, respectively). (B) Images for WF and GSD were overlaid individually for comparison (Bc for widefield and Bd for GSD). Overlaid signals from WF images (Bc) of nebulette and tropomyosin are significantly more diffuse than the sharp images obtained by GSD microscopy (Bd). Another cell (Be-Bh) elegantly illustrates the canonical desmin basket-weave network in the GSD image (Bf and Bh). This basket-weave pattern was originally observed by EM in the 1970's and 1980's (Wang and Ramirez-Mitchell, 1983). The exquisitely well-organized basket-like weave for desmin closely follows the nebulette puncta (Bh).

Supplemental Figure 5. To better visualize the decreased myofibril coverage for nebulette found in hearts from $Des^{-/-}$ mice, confocal z-sections were threaded in a sequential loop from top to bottom and vice versa. The intensity and number of nebulette striations throughout the myocardium of $Des^{-/-}$ mice was markedly reduced as compared to WT mice.